The Toll-like receptor-3 agonist poly(I:C) triggers nigrostriatal dopaminergic degeneration

Michela Deleidi[1], **Penelope J. Hallett**[1], **James B. Koprich**[1], **Chee-Yeun Chung**[1], and **Ole Isacson**[1,*]

[1] Center for Neuroregeneration Research, Harvard Medical School/McLean Hospital, Belmont, MA, 02478; Udall Parkinson's Disease Research Center of Excellence; Harvard Neurodiscovery Center, Boston, Massachusetts 02114

Abstract

In Parkinson's disease (PD), loss of striatal dopaminergic (DA) terminals and degeneration of DA neurons in the substantia nigra (SN) are associated with glial reactions. Such inflammatory processes are commonly considered an epiphenomenon of neuronal degeneration. However, there is increasing recognition of the role of neuroinflammation as an initiation factor of DA neuron degeneration. To investigate this issue, we established a new model of brain inflammation by injecting the Toll-like receptor 3 (TLR-3) agonist polyinosinic:polycytidylic acid [poly(I:C)] in the SN of adult rats. Poly(I:C) injection induced a sustained inflammatory reaction in the SN and in the dorsolateral striatum. Significant changes were detected in proteins relevant to synaptic transmission and axonal transport. In addition, cytoplasmic mislocalization of neuronal TDP-43 was observed. Poly(I:C) injection increased the susceptibility of midbrain DA neurons to a subsequent neurotoxic trigger (low dose 6-hydroxydopamine). Systemic delivery of IL-1 receptor antagonist (IL1-ra) protected SN DA neurons exposed to combined poly(I:C) induced inflammatory and neurotoxic oxidative stress.

These data indicate that viral-like neuroinflammation induces predegenerative changes in the DA system, which lowers the set point toward neuronal dysfunction and degeneration. New powerful neuroprotective therapies for PD might be considered by targeting critical inflammatory mechanisms, including cytokine-induced neurotoxicity.

Keywords

INTRODUCTION

Parkinson's disease (PD) is the second most common neurodegenerative disorder (Dauer and Przedborski, 2003). Most PD cases are sporadic, although many genetic mutations have been shown as causes or risk factors. The low penetrance of these mutations, and the low disease concordance in relatives suggest that there must be interactions between multiple risk factors (Farrer, 2006). The risk factors for PD include genetic predisposition, age and environmental triggers (Kasten et al., 2007). One such environmental stressor could be neuroinflammation. Activated microglia and high levels of proinflammatory molecules are

*Manuscript correspondence: Prof. Ole Isacson, Harvard Medical School/McLean Hospital, MRC 1, Belmont, MA 02478, Tel. 1-617-855-3283, Fax. 1-617-855-2522, ole_isacson@hms.harvard.edu.

present in the basal ganglia and brainstem of PD patients, 1-methyl-4-phenyl-1,2,3,6-tetrahydropyridine (MPTP) intoxicated patients, and in the basal ganglia in the 6-hydroxydopamine (6-OHDA), MPTP, and rotenone animal models of PD (McGeer et al., 1988; Langston et al., 1999; Liberatore et al., 1999; Cicchetti et al., 2002; Sherer et al., 2003). While these data suggest that inflammation is involved in PD progression, whether such inflammatory processes are pathogenic, or simply represent responses to neuronal degeneration, is unclear. Recent evidence suggests that neuroinflammation can be involved early in such disease processes and can be coupled with predegenerative changes in the dopaminergic (DA) system (Koprich et al., 2008; Chung et al., 2009). Several environmental triggers, including bacterial and viral infections, may initiate neuroinflammatory processes. It has been hypothesized that viruses have an etiological role in the development of several neurodegenerative disorders including PD (Mattson, 2004; Jang et al., 2009). Such a hypothesis is in line with the origin of post-encephalitic parkinsonism (Economo Von, 1931; Dale et al., 2004). Neurotropic viruses (e.g., arboviruses, influenza viruses, herpes viruses, JC virus, rotaviruses) may cause fulminant encephalitis, sometimes resulting in lethal consequences. More commonly, viruses enter the central nervous system (CNS) during subclinical infections, by the hematogenous route across the blood-brain barrier (BBB), or by the peripheral nerve route (Berth et al., 2009). Jang et al. showed that the intranasal administration of the neurotropic influenza virus H5N1 in mice triggers chronic microglia activation, phosphorylation and aggregation of α-synuclein (α-Syn) and a significant loss of DA in the SN (Jang et al., 2009). However, it is not clear whether the inflammatory reaction that accompanies subclinical CNS infections can initiate a degenerative process, or how inflammation can alter the normal neuronal function. Viral infections are indeed accompanied by a cytokine storm in the brain (Weller et al., 1991), and such inflammatory activation could be responsible for the CNS priming to degeneration and a possible aberrant response to subsequent neurotoxic triggers.

In order to investigate the role of neuroinflammatory processes induced by viral infections and the sensitization of DA neurons to neurotoxic triggers, we therefore developed a novel in vivo model of viral-like neuroinflammation. We injected the Toll-like receptor 3 (TLR-3) agonist polyinosinic:polycytidylic acid [poly(I:C)] into the SN of adult rats and characterized the cellular and molecular mechanisms underlying the resultant neuroinflammatory reaction. We then investigated whether these changes may hasten dysfunction of vulnerable nigral DA neurons, increasing their susceptibility to subsequent neurotoxic triggers.

MATERIAL AND METHODS

Animals

Female Sprague-Dawley rats weighing ~250 g (Charles River Laboratories, Wilmington, MA) were used in all animal experiments. All animal procedures were performed in accordance with current National Institutes of Health guidelines and McLean Hospital/Harvard University Institutional Animal Care and Use Committee protocols.

Stereotaxic injection of poly(I:C) into SN

All stereotaxic coordinates were derived from the Rat Atlas of Paxinos and Watson (Paxinos and Watson, 1986). For each surgery animals were deeply anesthetized with ketamine and xylazine (60 mg/kg and 3 mg/kg respectively, i.m.). Animals received a 4.0μl stereotaxic injection of poly(I:C) (total amount 10μg, 20 μg or 40 μg) (Axxora, San Diego, CA) delivered at a rate of 0.5 μl/min using microinfusion pumps (Stoelting Co, Wood Dale, IL) with a 5 minute wait time after injection. All injections were made into the SN using the

following anteroposterior (AP), mediolateral (ML), and dorsoventral (DV) coordinates: AP −5.5 mm, ML −2.0 mm, and DV 7.5 mm relative to dura. Toothbar (TB) set at − 3.3 mm.

6-OHDA intra-striatal injection

Animals received a single 3.5 μl stereotaxic injection of 6-OHDA (total dose = 5.0 μg of 6-OHDA prepared as free base, Sigma-Aldrich, St Louis, MO) delivered at a rate of 0.5 μl/min and a 5 min wait time after injection. Striatum injection coordinates were as follows: AP +0.2, ML −3.0, DV −5.0, and tooth bar set at −3.3.

Interleukin-1ra (IL-1ra) administration

Osmotic pumps (model 2ML1, Alzet, Cupertino, CA) were filled with either IL-1ra (Anakinra) (Amgen, Thousand Oaks, CA) (3.64 mg/kg/hr IL-1ra, s.c.) or vehicle and implanted subcutaneously. Pumps were replaced weekly until completion of the study.

Immunohistochemistry

Animals were terminally anesthetized by an intraperitoneal injection of sodium pentobarbital (100 mg/kg), and perfused intracardially with heparinized saline (0.1% heparin in 0.9% saline) followed by paraformaldehyde (4% in PBS). Immunohistochemical staining was performed as previously described (Bjorklund et al., 2002; Chung et al., 2009). The following primary antibodies were used: rabbit anti Iba1 (1:500, Wako, Chemical USA, Inc), rabbit anti GAD67 (1:5000, Sigma-Aldrich, Sigma-Aldrich, St Louis, MO), rabbit anti GFAP (1:1000, Dako, Carpinteria, CA), mouse anti MHC class II RT1B (1:100, AbD Serotec, UK), mouse anti CD68 1:100, AbD Serotec, UK), mouse anti CD11c (1:100, AbD Serotec, UK), mouse anti NMDAR1 (1:250, BD Transduction, CA), mouse anti NeuN (1:1000, Chemicon, International, Tamecula, CA), mouse anti PSD-95 (1:500, BD Transduction, CA), mouse anti TLR3/CD28 (1:50, Imgenex, San Diego, CA), rabbit anti TDP-43 (1:200, Abcam, Cambridge, MA), rabbit anti-tyrosine hydroxylase (TH) (Pel Freez; Rogers, AR, 1:1000). Sections were counterstained with Hoechst.

Stereological Procedures

Quantification of TH-positive neuronal number within the SN and VTA was performed by investigators blind to group treatments using an integrated Axioskop 2 microscope (Carl Zeiss, Thornwood, NY) and Stereo Investigator software (MBF Bioscience) and stereological principles as previously described (Chung et al., 2007) (Koprich et al., 2008). Briefly, SN and VTA were outlined by using the third cranial nerve as a landmark to define the vertical border between SN and VTA and by using the medial lemniscus as their dorsal border. The total number of TH-positive neurons was estimated from coded slides using the optical fractionator method. The number of sampling sites and other stereological parameters were experimentally determined to obtain a target coefficient of error (Gundersen's m = 1) of <0.10 for each case, thereby satisfying all criteria for objective stereological cell counts (Slomianka and West, 2005). Co-expression of Iba1/MHC-II was assessed in 5–7 random fields in all available sections from one series.

Optical Densitometry

Optical densitometry on TH-positive fibres in the striatum was performed using the NIH Image J software v1.3 (National Institutes of Health). For each animal, the average optical density of five separate sections through the striatum was determined. According to the atlas of Paxinos and Watson, the approximate sections were as follows relative to bregma: +0.22 mm, 0 mm, −0.26 mm, −0.74 mm, and −1.22 mm. Optical densitometry from a region of cortex immediately adjacent to the corpus callosum was used to correct striatal optical densitometry measurements for non-specific background.

Tissue preparation for Multiplex Elisa and Western blot analysis

Animals were terminally anesthetized the same way described above and perfused intracardially with heparinized saline (0.1% heparin in 0.9% saline). Striatum and SN were hand-dissected on ice-cold surface, assisted by a tissue chopper.

Multiplex ELISA

Tissue samples were homogenized in lysis buffer (TPER, Pierce, Rockford, IL) as previously described (Koprich et al., 2008). Halt protease and phosphatase inhibitor cocktail (1:100) was added fresh prior to cell lysis (Pierce, Rockford, IL). Samples were analyzed for the simultaneous detection of cytokines, chemokines and chemokine receptors using a multiplex ELISA based format and performed in duplicate (Pierce, Thermo Fisher Scientific, Woburn, MA) (Koprich et al., 2008).

Western blot analysis

Tissue samples were homogenized using hand-held Polytron homogenizer in ice-cold TEVP buffer, pH 7.4 [10 mM Tris–HCl, 5 mM NaF, 1 mM Na3VO4, 1 mM EDTA, 1 mM EGTA, 320 mM sucrose and protease inhibitors (Sigma P8340, 1:100)]. The homogenate was centrifuged at 800 x g to separate P1 (nuclear and debris) and supernatant (S1) fraction. S1 fraction was centrifuged at 9200 x g to separate P2 (membranous fraction) and S2 (cytosolic fraction). 10~20 μg of tissue proteins were used to run a gel. The respective volumes were mixed 1:1 with sample buffer and then boiled for 5 min. Samples were loaded into the Criterion precast 4~15%, 10%, or 12.5% SDS polyacryl-amide gel system (Bio-Rad). Proteins were transferred from the gel to a PVDF membrane electrically at 80 V for 1 h. Then, the membranes were washed in Tris-buffered saline with 0.1% Tween 20 (TBS-T). After at least 1 h of blocking in 5% nonfat dry milk, the membranes were incubated overnight at 4°C in various primary antibodies [CX3CR1 (Abcam, 1:500), Iba1 (Santa Cruz Biotechnology, 1:200), TLR-3 (Santa Cruz Biotechnology,1:200), α-Syn (BD Biosciences; 1:500), SNAP-25 (Millipore Bioscience Research Reagents; 1:2000), Rabphilin3A (BD Transduction Laboratories; 1:2000), RAB3B (Affinity Bioreagents; 1:2000), AMPA Receptor (GluR 2/3/4) (Cell Signaling;1:500), PSD-95 (Neuromab; 1:500), Drebrin (Genetex, 1:750), NMDAR1 (BD Transduction Laboratories; 1:400), SAP102 (Cell Signaling; 1:500), syntaxin (Millipore Bioscience Research Reagents; 1:1000), synaptophysin (Santa Cruz; 1:200), synaptotagmin (BD Transduction Laboratories; 1:1000), synapsin (Millipore Bioscience Research Reagents; 1:5000), Munc-18 (Affinity Bioreagents; 1:7500), KIF1A (clone 16, BD Transduction Laboratories; 1:2000), KIF1B (Novus Biologicals; 1:2000), KIF2A (Abcam; 1:10,000), KIF3A (Abcam; 1:2000), KIF5 (Abcam; 1:1000), KIF17 (Abcam; 1:1000), myosin Va (Sigma; 1:500), dynein (clone 74.1, Millipore Bioscience Research Reagents; 1:1000), dynamitin (Millipore Bioscience Research Reagents; 1:1000), α-tubulin (Affinity Bioreagents; 1:2000), β-tubulin (Covance; 1:5000), γ-tubulin (clone GTU-88, Sigma; 1:500), Actin (clone C-2, Santa Cruz; 1:500), and GAPDH (Millipore Bioscience Research Reagents; 1:5000)]. Then, the membranes were incubated in HRP-conjugated secondary antibodies for 1 h at room temperature. After washing with TBS-T, ECL or ECL plus (Amersham Biosciences) was used to probe for immunoreactive bands and exposed to film using the Hyblot film system (Denville Scientific). Optical density analysis (NIH ImageJ) was used to determine the relative abundance of protein in each sample.

Statistical analysis

The numbers of TH-IR positive neurons in the SN and VTA and optical density measurements of striatal TH fiber density were compared by one-way ANOVA followed by post hoc testing using Tukey's HSD method. Unpaired two-tailed t test applied at the 95%

confidence level (p < 0.05) was used to identify significantly different serum levels for each cytokine/chemokine and protein levels in rat SN and striatum, numbers of TH-IR neurons and TH fiber density in IL1b-ra experiment. Values of $P < 0.05$ were accepted as statistically significant. The Statistical Package GraphPad Prism version 4.00 (GraphPad Software, San Diego California USA) was used to analyze the data.

RESULTS

The injection of the Toll-like receptor 3 (TLR-3) agonist poly(I:C) induces a long-lasting inflammatory reaction in the SN and dorsolateral striatum

To mimic the neuroinflammatory cascade elicited by a viral infection, we injected the TLR-3 agonist poly(I:C) into the substantia nigra pars compacta (SNc) of adult Sprague Dawley rats. We first determined the optimal dose of poly(I:C) that provided a neuroinflammatory response without inducing tyrosine hydroxylase-immunoreactive (TH-ir) cell loss. Sprague-Dawley rats were injected with different doses of poly(I:C) (10, 20, and 40 μg) in the SNc. We examined the neuroinflammatory reaction by immunohistochemical analysis using Iba1 as a marker of microglia and we quantified DA cell loss by TH-ir cell counting in the SNc at 12 days after injection. The intranigral injection of poly(I:C) induced microglial activation in a dose-dependant manner, as revealed by greater Iba1 immunostaining in animals injected with higher doses (data not shown). The injection of 40 μg of poly(I:C) produced significant TH-ir cell loss within the SNc (data not shown), while lower doses (10 and 20 μg) did not induce significant cell loss.

To examine the time course of poly(I:C)-induced neuroinflammatory reaction, animals were injected with 20 μg poly(I:C) in the SNc and the degree of microglial activation was determined by Iba1 immunostaining at 4, 12 and 33 days after the injection. It has been reported that the intracerebroventricular injection of poly(I:C) in mice induces robust microglia activation in the cereberal cortex via TLR-3 activation (Town et al., 2006). The intranigral injection of poly(I:C) induced microglial activation as shown by the presence of Iba1 immunoreactive cells with rod-like morphology as early as 4 days after the injection, which subsequently peaked at 12 days and persisted for 33 days (Fig. 1A–D). Immunostaining for OX6 [a monomorphic determinant of the rat major histocompatibility complex (MHC) class II antigen, expressed by activated microglial cells] confirmed the persistent microglial activation after the intranigral injection of poly(I:C) (Supplementary Figure 1A). We found that 25% of Iba1$^+$ cells coexpressed MHC-II antigen 12 days after poly(I:C) injection (Supplementary Figure 1A). Many MHC-II$^+$ cells were found in the perivascular areas. We further characterized the microglial reaction using antibodies against the macrophage marker CD68 and dendritic cell marker CD11c. Poly(I:C) injection induced activation of perivascular and parenchymal CD68$^+$ macrophages (Supplementary Figure 1C–D). Interestingly, many perivascular CD11c$^+$/Iba1$^+$ cells were detected after poly(I:C) injection, suggesting dendritic cell activation (Supplementary Figure 1B). A few parenchymal CD11c$^+$ cells were also detected after poly(I:C) injection (Supplementary Figure 1B). We did not detect T cell infiltration in brains of rats injected with poly(I:C). The neuroinflammatory response was quantified by western blot analysis, which showed increased levels of Iba1, TLR-3 and the fractalkine receptor, CX3CR1, in the SN at 12 days after poly(I:C) injection (Fig. 2I). We next examined astrocytic activation by glial fibrillary acidic protein (GFAP) immunostaining in both groups of rats following administration of either poly(I:C) or vehicle. At 12 days after injection, the GFAP immunoreactivity was increased in the SN of animals injected with poly(I:C) when compared to control animals. Astrocytic activation was still evident in the SN 33 days after poly(I:C) injection (Fig. 1I–L). Interestingly, the intranigral injection of poly(I:C) induced a neuroinflammatory response in the dorsolateral striatum. Starting at 12 days after poly(I:C) injection, Iba1 positive microglia in the dorsolateral striatum showed an activated phenotype as evident by

their larger soma with short swollen processes compared with the elongated and needle-like shape in the control animals (Fig. 2A–C). Striatal microglial activation decreased over time and returned to baseline conditions 33 days after the injection (Fig. 2D). Microglia activation was quantified by western blot analysis, which revealed higher levels of Iba1 in the dorsolateral striatum of rats 12 days after poly(I:C) injection (Fig. 2J). In parallel, we found a long-lasting astrocytic reaction starting at 12 days after the injection, which persisted up to 33 days (Fig. 2E–H).

Poly(I:C) is a synthetic double strand RNA (dsRNA) which selectively binds to TLR-3 (Alexopoulou et al., 2001), an innate immune receptor expressed in neurons, microglia and astrocytes (Bsibsi et al., 2002). Our analysis revealed that TLR-3 was highly expressed in DA neurons within the SNc and in ventral tegmental area (VTA) in control animals (Supplementary Fig. 2A). In contrast, microglia and astrocytes expressed lower level of TLR-3 (Supplementary Fig. 2C,E). Poly(I:C) injection resulted in an upregulation of TLR-3 in neurons at 12 days after the injection (Supplementary Fig. 2B), whereas microglia and astrocytes showed a moderate upregulation (Supplementary Fig. 2D–F). Western blot analysis confirmed increased levels of TLR-3 in the SN of poly(I:C) injected animals 12 days after the injection, while striatal levels remained unchanged (Fig. 3I–J).

The intranigral injection of poly(I:C) increases the level of proinflammatory cytokines and chemokines in the SN and striatum

To profile the neuroinflammatory response to poly(I:C), we measured the protein level of pro-inflammatory cytokines and chemokines in the SN and in the dorsolateral striatum of rats at 12 days after the injection using Multiplex Elisa assay. We chose this time point since, as revealed by our immunohistochemical analysis (Figure 1,2), both the poly(I:C)-injected SN and the dorsolateral striatum showed robust astrocytic and microglia activation at 12 days after poly (I:C) injection. In addition, mouse models of viral infections and human pathology show that active viral infections lasts approximately 10 days (Jang et al., 2009b) (de Jong et al., 2005). Therefore this time point most closely mimics post-acute viral infections when immune reactions may persist within the brain parenchyma in the absence of viral particles. Our analysis revealed that in the SN, the levels of IL-1α and the chemokines MCP-1 and RANTES were significantly elevated (Table 1; t=2.194, p<0.05; t=2.179, p<0.05; t=3.846, p<0.01 respectively) while IL1-β, IL-6, TNF-α, MCP-1 and TGF-β1 were elevated in the dorsolateral striatum (Table 1; t=2.962, p<0.01; t=2.164, p<0.05; t=2.590, p<0.05; t=2.494, p<0.01; t=3.838, p<0.01; respectively).

The intranigral injection of poly(I:C) alters the expression of axonal and synaptic proteins in the SN and striatum

To investigate whether poly(I:C) injection influenced neuronal properties and synaptic function, we measured the levels of various axonal and synaptic proteins in the SN and in the dorsolateral striatum at 12 days after injection. Among axonal transport proteins, levels of anterograde transport motor proteins (KIF1A, KIF1B) were increased in the SN, while KIF3A and KIF17 were reduced (Fig. 3A–B). Levels of dynein, a retrograde transport motor protein, were also decreased (Fig. 3A–B). In the dorsolateral striatum, we found decreased levels of KIF17 (Fig 4A–B). Cytoskeletal protein (actin, α-Tubulin, β-Tubulin and γ-Tubulin) levels were not altered by the intranigral injection of poly(I:C) (Fig. 3,4). Among synaptic proteins, RAB3B and α-Syn levels were decreased in the SN (Fig. 5A–B). In the dorsolateral striatum levels of the postsynaptic scaffold PSD-95 and NMDA receptor subunit 1 (NR1) were increased while levels of RAB3B, MUNC18, drebrin and SAP102 were reduced (Fig. 6A–B). Overexpression of PSD-95 and NR1 was confirmed by immunohistochemistry, showing that synaptic PSD-95 and NR1 staining was more intense in the striatum of poly(I:C)-injected animals (Supplementary Fig. 2G-J).

Poly(I:C) injection induces cytosolic mislocalization of neuronal TDP-43

Levels of TAR DNA binding protein (TDP-43) were increased in the SN and decreased in the dorsolateral striatum 12 days after the injection (Fig. 3,4). We therefore analysed the effect of poly(I:C) injection on the subcellular localization of TDP-43. In vehicle-injected animals, TDP-43 was largely restricted to the nucleus whereas diffuse cytoplasmic TDP-43 neuronal staining was observed in the SN after poly(I:C) injection (Supplementary Fig. 2K–N). Neither intranuclear nor cytoplasmic TDP-43-immunoreactive protein aggregates were detected.

The TLR-3 agonist poly(I:C) increases vulnerability to nigral DA neuron loss induced by low-dose 6-OHDA

To test the hypothesis that viral-like neuroinflammation induced by the TLR-3 agonist poly(I:C) increases the vulnerability of the DA nigrostriatal system to degeneration, we injected rats with 20 μg poly(I:C) followed after 12 days by an intra-striatal injection of a low-dose of 6-OHDA (5 μg). Neuronal cell loss was analyzed 21 days after the injection of 6-OHDA (Fig. 7A). We previously reported the use of low-dose 6-OHDA in combination with the bacterial mimic lipopolysaccharide (LPS) in a double-hit model of DA neuron degeneration (Koprich et al., 2008). This allows the investigation of the combined role of neuroinflammation and neurotoxic triggers in the onset of DA neuron degeneration. Unbiased stereological analyses of TH-ir neurons within the SN revealed that intranigral poly(I:C) followed by intra-striatal injection of low dose 6-OHDA produced a greater TH-ir cell loss compared to the injection of low-dose 6-OHDA alone (Fig. 7B, F-G and Supplementary Figure 3A; 3011 ± 332 and 5020 ± 492 respectively; $p<0.05$). Stereological counts of NeuN-immunopositive neurons further confirmed this neuronal loss (Fig. 7B, 7J–K and Supplementary Figure 3A; 9238 ± 320 and 15893 ± 1297, respectively; $p<0.01$). Either vehicle or poly(I:C) alone did not induced significant cell loss (Figure 7B, D-E, 7H–I and Supplementary Figure 3A. TH^+ cells: 6952.3 ± 345 and 6783.3 ± 515, respectively. $NeuN^+$ cells 22684.9 ± 1171 and 25042.9 ± 1923, respectively). Unbiased stereological analysis indicated no loss of TH-positive or NeuN-positive neurons in the VTA in any of the groups [Fig. 7C and Supplementary Figure 3B. TH^+ cells: vehicle alone (9523 ± 1228), poly(I:C)/ vehicle (9138.8 ± 659), vehicle/6-OHDA (8984.7 ± 543), poly(I:C)/6-OHDA (9638.5 ± 1165); $NeuN^+$ cells: vehicle alone (12500 ± 1234), poly(I:C)/vehicle (12477.3 ± 2000), vehicle/6-OHDA (13368.9 ± 1799), poly(I:C)/6-OHDA (11414.1 ± 1254)]. Moreover, the different treatments [poly(I:C), low-dose 6-OHDA, poly(I:C) followed by low-dose 6-OHDA] did not alter the qualitative expression pattern of GAD67 staining, either in cell bodies or presynaptic terminal density (Supplementary Figure 4G–I). It is therefore likely that DA neurons of the SNpc are selectively vulnerable to the actions of inflammatory stimuli. We then compared the neuroinflammatory and astrocytic reaction in animals injected with low-dose 6-OHDA alone, and in the combined insult model. Neuronal cell loss was accompanied by microgliosis and astrocytic activation within the SN in both groups (Supplementary Figure 4A–F). However, microglial activation as assessed by Iba1 immunohistochemistry was prominent in animals injected with poly(I:C) followed by low-dose 6-OHDA (Supplementary Figure 4A–C). In parallel, animals injected with poly(I:C) and 6-OHDA displayed a more prominent astrocytic activation when compared to animals injected with 6-OHDA alone (Supplementary Figure 4D–F).

Intranigral injection of poly(I:C) increases the susceptibility of dopaminergic nerve terminals in the striatum to 6-OHDA toxicity

To investigate whether poly(I:C) injection produced changes in the striatal DA terminals in response to 6-OHDA neurotoxicity, we stained striatal sections for TH and performed densitometric analysis. TH immunostaining through the striatum revealed a marked reduction in DA innervation on the side ipsilateral to the combined 6-OHDA and poly(I:C)/

6-OHDA lesion compared to the intact hemisphere (Fig. 8A–D). Densitometric quantification of TH-positive fibres showed a significant reduction in animals injected with 6-OHDA alone or poly(I:C) followed by a subtoxic dose of 6-OHDA compared to control animals ($79.1 \pm 4.9\%$, $64.5 \pm 3.7\%$, $97.9 \pm 1.8\%$ of the contralateral side, $p<0.001$ and $p<0.01$ respectively) (Fig. 8E). There was a significant reduction of TH density in animals injected with poly(I:C) followed by 6-OHDA compared to animals injected with 6-OHDA alone ($p<0.05$) (Fig. 8E). TH fibres were preserved in the striatum of rats injected with poly(I:C) alone ($95.4 \pm 7.3\%$ of the contralateral side) (Fig 8B,E). These data indicate that poly(I:C) injection increases the vulnerability of TH terminals in the striatum to 6-OHDA toxicity. Iba1 immunohistochemistry revealed activated microglial cells within the dorsolateral striatum of animals injected with 6-OHDA alone or poly(I:C)/6-OHDA (Fig. 8F–G). However, the microglial reaction was more prominent in animals injected with poly(I:C) combined with low-dose of 6-OHDA (Fig. 8G). Hypertrophied, activated GFAP+ astrocytes were detected in the dorsolateral striatum of both groups (Fig. 8H–I).

Neutralization of IL-1 reduces cell loss produced by poly(I:C) and 6-OHDA

The intranigral injection of poly(I:C) induced an upregulation of IL-1 in the SN and in the dorsolateral striatum (Table 1). The pro-inflammatory cytokine IL-1 has been implicated as a central mediator of acute neuronal loss in experimental studies and in chronic neurodegenerative disorders (Allan et al., 2005). To investigate the potential role of IL-1 in the poly(I:C)-induced sensitization of the nigrostriatal DA system, we analysed whether interleukin 1 receptor antagonist (IL1ra) treatment prevented the degeneration produced by the combination of poly(I:C) and 6-OHDA. Importantly, IL1-ra has already been used in clinical settings with minor side effects and it can be systemically delivered with favorable kinetics in crossing BBB (Fisher et al., 1994;Nuki et al., 2002;Clark et al., 2008). All animals received an intra-nigral injection of poly(I:C), followed by the subcutaneous infusion of either IL-1ra (n=12) or vehicle (n=11) from day 9 until sacrifice and, finally, all animals received an intra-striatal injection of 5 μg 6-OHDA on day 12 (Fig. 9A). Post-mortem analysis revealed that IL1-ra significantly prevented TH-ir cell death in the SN when compared to vehicle treated controls (2916.111 ± 972.034 and 5734.3 ± 601.275; $p < 0.01$] (Fig. 9B,C,F) and TH-fiber loss ($91.34 \pm 4.8\%$ and $68.95 \pm 4.5\%$ of the contralateral side respectively, $p < 0.01$) in the dorsolateral striatum (Fig. 9D,E,G). These data indicate that blocking IL-1 signaling significantly reduces the degree of degeneration produced by the combination of poly(I:C) and 6-OHDA.

DISCUSSION

In this study we developed a new model of neuroinflammation by the intra-parenchymal injection of the TLR-3 agonist poly(I:C). This model reproduces the activation of the brain innate immune system occurring during non-cytopathic CNS viral infections. We demonstrated that such neuroinflammatory responses activated a cascade of events (changes in the levels of proteins relevant to axonal transport and synaptic transmission, neuronal TDP-43 cytoplasmic mislocalization), which reflect the changes observed in early neurodegenerative stages. The activation of the brain innate immunity primed the nigrostriatal DA system to oxidative stress-induced degeneration. Importantly, IL1-ra attenuated degeneration in this model, confirming the neurotoxic role of cytokines.

The relationship between neurodegeneration and inflammation in PD remains largely unknown. One intriguing hypothesis is that environmental stressors activate brain immune cells, which then cause or contribute to the degeneration of vulnerable neuronal populations, such as the DA neurons of the nigrostriatal system (Perry, 2004). Inflammation in the CNS can be initiated by immunological stimuli, such as bacterial or viral infections (Kreutzberg, 1996). Genetic susceptibility can also accelerate nigral DA neuron loss in response to

inflammatory triggers (Frank-Cannon et al., 2008; Gao et al., 2008). In a theoretical framework, the fact that all humans experience bacterial and viral infections, suggest that such inflammatory processes can contribute to the well-known age associated aggregate risk of PD in susceptible individuals (de Lau and Breteler, 2006). Peripheral immune responses generate inflammatory mediators that alter BBB permeability allowing viruses to enter the CNS (Wang et al., 2004). Viruses can induce CNS dysfunction by direct cytolytic effect or by-stander inflammatory reactions (van den Pol, 2006).

Poly(I:C)-induced long-lasting neuroinflammatory response in the SN and dorsolateral striatum

The intranigral injection of poly(I:C) induced a sustained neuroinflammatory reaction in the SN and in the dorsolateral striatum. Such a propagation of inflammatory responses could be important in neurodegenerative conditions as a contributor to the progressive damage (Cagnin et al., 2001; Cicchetti et al., 2002). This propagation could be explained by the result of glial-glial as well as neuron-glia communication mechanisms (Giaume et al.). Focal neuronal demise can result in widespread astrocytic glial reactions, which follow the anatomical connectivity of the lesioned area (Isacson et al., 1987; de Jong et al., 2005). This hypothesis could include an inflammatory response propagated by DA neurons in the SN, which were triggered by poly(I:C) and released pro-inflammatory molecules at the axon terminals in the striatum. In line with this evidence, poly(I:C) injection induced an up-regulation of TLR-3 that was more prominent in neurons.

Poly(I:C)-induced changes in levels of proteins involved in synaptic transmission and axonal transport

Our study shows that a viral challenge results in important changes in the levels of synaptic and axonal transport proteins in the absence of overt neurodegeneration. Notably, similar defects precede DA neuron degeneration and are coupled with neuroinflammation in a rat model of α-synucleinopathy (Chung et al., 2009). The most significant change was the increase of the postsynaptic proteins PSD-95 and NMDAR1 in the dorsolateral striatum. Increase in the expression of PSD-95 has been reported in the entorhinal and frontal cortex of Alzheimer's disease (AD) patients (Leuba et al., 2008). These changes could be due to compensatory mechanisms related to the reduced levels of pre-synaptic proteins implicated in synaptic transmission and exocytosis (RAB3B and MUNC18), or to an altered subcellular distribution. In this study we show that axonal transport proteins are also altered after poly(I:C) injection. Therefore PSD-95 and other spine proteins could accumulate in the dendritic shafts, showing a pattern of abnormal distribution and increased density. Importantly, a decrease of drebrin was found in the dorsolateral striatum. Drebrin A is an actin-binding protein specifically localized at dendritic spines of mature neurons and plays a role in synaptic function and spinous clustering of PSD-95 (Takahashi et al., 2003; Aoki et al., 2005). A major loss of drebrin A in dendritic spines has been reported in patients with AD, Down's syndrome and aging (Harigaya et al., 1996; Hatanpaa et al., 1999; Shim and Lubec, 2002).

Defects in axonal transport can be early pathogenic events in many human neurodegenerative diseases (Morfini et al., 2009). Our study revealed that anterograde transport motor proteins that carry synaptic vesicles (KIF1A, KIF1B) were markedly elevated in the SN. Other cargo containing vesicles (KIF3A and KIF17) to synaptic terminals were markedly reduced. In parallel, we found a significant decrease of KIF17 in the dorsolateral striatum. Levels of the retrograde transport microtubule motor protein, dynein, were decreased in the SN. Interestingly, loss of dynein function results in the misaccumulation of synaptic proteins and has been linked to neurodegeneration (Koushika

et al., 2004; Banks and Fisher, 2008). This could explain the reduction of presynaptic proteins described in our model.

In summary, our findings provide evidence that a viral challenge induces changes of proteins involved in synaptic transmission and axonal transport, which reflect the early stages of human neurodegenerative diseases. This suggests that viral-mediated neuronal dysfunction may be casually linked to the onset of neurodegeneration.

Given the expression of TLR-3 on microglia, astrocytes and neurons (Bsibsi et al., 2002), future studies will investigate whether such changes directly correlate with neuronal TLR-3 activation rather than with by-stander inflammatory reactions.

Poly(I:C)-induced cytosolic mislocalization of neuronal TDP-43

The axonal transport changes observed after poly(I:C) injection were coupled with an accumulation of TDP-43 in the dorsolateral striatum and a decrease of this protein in the SN. TDP-43 pathology has been identified in 19% of PD dementia, and 7% of PD cases (Nakashima-Yasuda et al., 2007). However, it is not clear whether TDP-43 has a physiological role in the response to neuronal injury and whether inflammation may alter its function. Our studies demonstrate that poly(I:C) injection induces TDP-43 redistribution to the neuronal cytosol in the absence of pathological aggregates. The increase of TDP-43 levels in the dorsolateral striatum after poly(I:C) injection could occur as a consequence of the impairment of the axonal transport machinery. Alternatively, one cannot exclude that a defective autophagic clearance could contribute to TDP-43 redistribution and accumulation.

Poly(I:C)-induced sensitization lowers threshold to neurotoxic triggers

Poly(I:C) delivered to the SN prior to the intra-striatal injection of a low dose of 6-OHDA produced an increase of DA cell death. These data support the hypotheses that neuroinflammation exerts a sensitizing action on the brain inducing an aberrant response to subsequent neurotoxic challenges. Brain microglia, which were persistently activated after poly(I:C) injection, could react to 6-OHDA injection with an abnormal release of neurotoxic mediators. We also hypothesize that the initial neuroinflammatory reaction and neuronal TLR-3 activation elicited by the viral challenge may exert a priming action directly on neurons rendering them more vulnerable to external stressors. This reasoning is suggested by the prominent upregulation of neuronal TLR-3 after poly (I:C) injection. Interestingly, TLR-3 is a negative regulator of embryonic neural progenitor cell proliferation and neurite extension (Cameron et al., 2007; Lathia et al., 2008).

IL1-ra neuroprotective effect against combined inflammatory and neurotoxic oxidative stress

Inhibition of IL1 signaling by systemic administration of IL-1ra prevented the increased vulnerability produced by poly(I:C) and eliminated its contribution to 6-OHDA induced DA cell death. IL-1β is one of the key proinflammatory cytokines in neurodegeneration (Allan et al., 2005). Importantly, IL-1ra can cross the BBB with favorable kinetics and it has proved safe in patients with sepsis, rheumatoid arthritis and subarachnoid hemorrhage (Fisher et al., 1994; Clark et al., 2008) (Nuki et al., 2002). Notably, IL-1ra determines a significantly decrease of TNF-α levels, a pro-inflammatory cytokine that plays a key role in DA neuron degeneration (Koprich et al., 2008) (McCoy et al., 2008). We therefore believe that IL-1ra may exert its neuroprotective action through multiple mechanisms including blockade of IL-1 signaling, but also regulating other cytokines such as TNF-α.

NIH-PA Author Manuscript

Summary and conclusion

We have developed a new model of neuroinflammation by the intra-parenchymal injection of the TLR-3 agonist poly(I:C), and performed a systematic analysis of the pathophysiological changes occurring in the DA nigrostriatal system. Our data show that the brain innate immune responses triggered by TLR-3 activation can initiate a cascade of neurodegenerative events, which reflect the changes described in the earliest stages in animal models of DA neuron degeneration (Chung et al., 2009). Overall, these data support the hypothesis that neuroinflammation plays a critical role in priming vulnerable neuronal populations to degeneration. DA midbrain neurons are highly sensitive to inflammatory "stressors", and, over a lifetime, such neuroinflammatory events could substantially increase the number of potential degenerative changes. Based on these data, new neuroprotective therapies can be examined by targeting critical inflammatory mechanisms and molecules such as cytokines. In view of the beneficial and detrimental effects of neuroinflammation (Town et al., 2005) (Colton and Wilcock), the challenging goal will be to develop immunomodulatory interventions that can restore the homeostatic level of the immune system harnessing its neuroprotective arm.

Supplementary Material

Refer to Web version on PubMed Central for supplementary material.

Acknowledgments

References

Alexopoulou L, Holt AC, Medzhitov R, Flavell RA. Recognition of double-stranded RNA and activation of NF-kappaB by Toll-like receptor 3. Nature. 2001; 413:732–738. [PubMed: 11607032]

Allan SM, Tyrrell PJ, Rothwell NJ. Interleukin-1 and neuronal injury. Nat Rev Immunol. 2005; 5:629–640. [PubMed: 16034365]

Aoki C, Sekino Y, Hanamura K, Fujisawa S, Mahadomrongkul V, Ren Y, Shirao T. Drebrin A is a postsynaptic protein that localizes in vivo to the submembranous surface of dendritic sites forming excitatory synapses. J Comp Neurol. 2005; 483:383–402. [PubMed: 15700273]

Banks GT, Fisher EM. Cytoplasmic dynein could be key to understanding neurodegeneration. Genome Biol. 2008; 9:214. [PubMed: 18373888]

Berth SH, Leopold PL, Morfini GN. Virus-induced neuronal dysfunction and degeneration. Front Biosci. 2009; 14:5239–5259. [PubMed: 19482613]

Bjorklund LM, Sanchez-Pernaute R, Chung S, Andersson T, Chen IY, McNaught KS, Brownell AL, Jenkins BG, Wahlestedt C, Kim KS, Isacson O. Embryonic stem cells develop into functional dopaminergic neurons after transplantation in a Parkinson rat model. Proc Natl Acad Sci U S A. 2002; 99:2344–2349. [PubMed: 11782534]

Bsibsi M, Ravid R, Gveric D, van Noort JM. Broad expression of Toll-like receptors in the human central nervous system. J Neuropathol Exp Neurol. 2002; 61:1013–1021. [PubMed: 12430718]

Cagnin A, Brooks DJ, Kennedy AM, Gunn RN, Myers R, Turkheimer FE, Jones T, Banati RB. In-vivo measurement of activated microglia in dementia. Lancet. 2001; 358:461–467. [PubMed: 11513911]

Cameron JS, Alexopoulou L, Sloane JA, DiBernardo AB, Ma Y, Kosaras B, Flavell R, Strittmatter SM, Volpe J, Sidman R, Vartanian T. Toll-like receptor 3 is a potent negative regulator of axonal growth in mammals. J Neurosci. 2007; 27:13033–13041. [PubMed: 18032677]

Chung CY, Koprich JB, Endo S, Isacson O. An endogenous serine/threonine protein phosphatase inhibitor, G-substrate, reduces vulnerability in models of Parkinson's disease. J Neurosci. 2007; 27:8314–8323. [PubMed: 17670978]

Chung CY, Koprich JB, Siddiqi H, Isacson O. Dynamic changes in presynaptic and axonal transport proteins combined with striatal neuroinflammation precede dopaminergic neuronal loss in a rat model of AAV alpha-synucleinopathy. J Neurosci. 2009; 29:3365–3373. [PubMed: 19295143]

Cicchetti F, Brownell AL, Williams K, Chen YI, Livni E, Isacson O. Neuroinflammation of the nigrostriatal pathway during progressive 6-OHDA dopamine degeneration in rats monitored by immunohistochemistry and PET imaging. Eur J Neurosci. 2002; 15:991–998. [PubMed: 11918659]

Clark SR, McMahon CJ, Gueorguieva I, Rowland M, Scarth S, Georgiou R, Tyrrell PJ, Hopkins SJ, Rothwell NJ. Interleukin-1 receptor antagonist penetrates human brain at experimentally therapeutic concentrations. J Cereb Blood Flow Metab. 2008; 28:387–394. [PubMed: 17684519]

Colton CA, Wilcock DM. Assessing activation states in microglia. CNS Neurol Disord Drug Targets. 9:174–191. [PubMed: 20205642]

Dale RC, Church AJ, Surtees RA, Lees AJ, Adcock JE, Harding B, Neville BG, Giovannoni G. Encephalitis lethargica syndrome: 20 new cases and evidence of basal ganglia autoimmunity. Brain. 2004; 127:21–33. [PubMed: 14570817]

Dauer W, Przedborski S. Parkinson's disease: mechanisms and models. Neuron. 2003; 39:889–909. [PubMed: 12971891]

de Jong EK, Dijkstra IM, Hensens M, Brouwer N, van Amerongen M, Liem RS, Boddeke HW, Biber K. Vesicle-mediated transport and release of CCL21 in endangered neurons: a possible explanation for microglia activation remote from a primary lesion. J Neurosci. 2005; 25:7548–7557. [PubMed: 16107642]

de Lau LM, Breteler MM. Epidemiology of Parkinson's disease. Lancet Neurol. 2006; 5:525–535. [PubMed: 16713924]

Economo Von, C. Encephalytis Lethargica: its Sequelae and Treatment. Oxford University Press; London: 1931.

Farrer MJ. Genetics of Parkinson disease: paradigm shifts and future prospects. Nat Rev Genet. 2006; 7:306–318. [PubMed: 16543934]

Fisher CJ Jr, Dhainaut JF, Opal SM, Pribble JP, Balk RA, Slotman GJ, Iberti TJ, Rackow EC, Shapiro MJ, Greenman RL, et al. Recombinant human interleukin 1 receptor antagonist in the treatment of patients with sepsis syndrome. Results from a randomized, double-blind, placebo-controlled trial. Phase III rhIL-1ra Sepsis Syndrome Study Group. Jama. 1994; 271:1836–1843. [PubMed: 8196140]

Frank-Cannon TC, Tran T, Ruhn KA, Martinez TN, Hong J, Marvin M, Hartley M, Trevino I, O'Brien DE, Casey B, Goldberg MS, Tansey MG. Parkin deficiency increases vulnerability to inflammation-related nigral degeneration. J Neurosci. 2008; 28:10825–10834. [PubMed: 18945890]

Gao HM, Kotzbauer PT, Uryu K, Leight S, Trojanowski JQ, Lee VM. Neuroinflammation and oxidation/nitration of alpha-synuclein linked to dopaminergic neurodegeneration. J Neurosci. 2008; 28:7687–7698. [PubMed: 18650345]

Giaume C, Koulakoff A, Roux L, Holcman D, Rouach N. Astroglial networks: a step further in neuroglial and gliovascular interactions. Nat Rev Neurosci. 11:87–99. [PubMed: 20087359]

Harigaya Y, Shoji M, Shirao T, Hirai S. Disappearance of actin-binding protein, drebrin, from hippocampal synapses in Alzheimer's disease. J Neurosci Res. 1996; 43:87–92. [PubMed: 8838578]

Hatanpaa K, Isaacs KR, Shirao T, Brady DR, Rapoport SI. Loss of proteins regulating synaptic plasticity in normal aging of the human brain and in Alzheimer disease. J Neuropathol Exp Neurol. 1999; 58:637–643. [PubMed: 10374754]

Isacson O, Fischer W, Wictorin K, Dawbarn D, Bjorklund A. Astroglial response in the excitotoxically lesioned neostriatum and its projection areas in the rat. Neuroscience. 1987; 20:1043–1056. [PubMed: 3601061]

Jang H, Boltz D, Sturm-Ramirez K, Shepherd KR, Jiao Y, Webster R, Smeyne RJ. Highly pathogenic H5N1 influenza virus can enter the central nervous system and induce neuroinflammation and neurodegeneration. Proc Natl Acad Sci U S A. 2009; 106:14063–14068. [PubMed: 19667183]

Kasten M, Chade A, Tanner CM. Epidemiology of Parkinson's disease. Handb Clin Neurol. 2007; 83:129–151. [PubMed: 18808913]

Koprich JB, Reske-Nielsen C, Mithal P, Isacson O. Neuroinflammation mediated by IL-1beta increases susceptibility of dopamine neurons to degeneration in an animal model of Parkinson's disease. J Neuroinflammation. 2008; 5:8. [PubMed: 18304357]

Koushika SP, Schaefer AM, Vincent R, Willis JH, Bowerman B, Nonet ML. Mutations in Caenorhabditis elegans cytoplasmic dynein components reveal specificity of neuronal retrograde cargo. J Neurosci. 2004; 24:3907–3916. [PubMed: 15102906]

Kreutzberg GW. Microglia: a sensor for pathological events in the CNS. Trends Neurosci. 1996; 19:312–318. [PubMed: 8843599]

Langston JW, Forno LS, Tetrud J, Reeves AG, Kaplan JA, Karluk D. Evidence of active nerve cell degeneration in the substantia nigra of humans years after 1-methyl-4-phenyl-1,2,3,6-tetrahydropyridine exposure. Ann Neurol. 1999; 46:598–605. [PubMed: 10514096]

Lathia JD, Okun E, Tang SC, Griffioen K, Cheng A, Mughal MR, Laryea G, Selvaraj PK, ffrench-Constant C, Magnus T, Arumugam TV, Mattson MP. Toll-like receptor 3 is a negative regulator of embryonic neural progenitor cell proliferation. J Neurosci. 2008; 28:13978–13984. [PubMed: 19091986]

Leuba G, Savioz A, Vernay A, Carnal B, Kraftsik R, Tardif E, Riederer I, Riederer BM. Differential changes in synaptic proteins in the Alzheimer frontal cortex with marked increase in PSD-95 postsynaptic protein. J Alzheimers Dis. 2008; 15:139–151. [PubMed: 18780974]

Liberatore GT, Jackson-Lewis V, Vukosavic S, Mandir AS, Vila M, McAuliffe WG, Dawson VL, Dawson TM, Przedborski S. Inducible nitric oxide synthase stimulates dopaminergic neurodegeneration in the MPTP model of Parkinson disease. Nat Med. 1999; 5:1403–1409. [PubMed: 10581083]

Mattson MP. Infectious agents and age-related neurodegenerative disorders. Ageing Res Rev. 2004; 3:105–120. [PubMed: 15163105]

McCoy MK, Ruhn KA, Martinez TN, McAlpine FE, Blesch A, Tansey MG. Intranigral lentiviral delivery of dominant-negative TNF attenuates neurodegeneration and behavioral deficits in hemiparkinsonian rats. Mol Ther. 2008; 16:1572–1579. [PubMed: 18628756]

McGeer PL, Itagaki S, Boyes BE, McGeer EG. Reactive microglia are positive for HLA-DR in the substantia nigra of Parkinson's and Alzheimer's disease brains. Neurology. 1988; 38:1285–1291. [PubMed: 3399080]

Morfini GA, Burns M, Binder LI, Kanaan NM, LaPointe N, Bosco DA, Brown RH Jr, Brown H, Tiwari A, Hayward L, Edgar J, Nave KA, Garberrn J, Atagi Y, Song Y, Pigino G, Brady ST. Axonal transport defects in neurodegenerative diseases. J Neurosci. 2009; 29:12776–12786. [PubMed: 19828789]

Nakashima-Yasuda H, Uryu K, Robinson J, Xie SX, Hurtig H, Duda JE, Arnold SE, Siderowf A, Grossman M, Leverenz JB, Woltjer R, Lopez OL, Hamilton R, Tsuang DW, Galasko D, Masliah E, Kaye J, Clark CM, Montine TJ, Lee VM, Trojanowski JQ. Co-morbidity of TDP-43 proteinopathy in Lewy body related diseases. Acta Neuropathol. 2007; 114:221–229. [PubMed: 17653732]

Nuki G, Bresnihan B, Bear MB, McCabe D. Long-term safety and maintenance of clinical improvement following treatment with anakinra (recombinant human interleukin-1 receptor antagonist) in patients with rheumatoid arthritis: extension phase of a randomized, double-blind, placebo-controlled trial. Arthritis Rheum. 2002; 46:2838–2846. [PubMed: 12428223]

Paxinos, G.; Watson, C. The rat brain in stereotaxic coordinates. 2. San Diego: Academic; 1986.

Perry VH. The influence of systemic inflammation on inflammation in the brain: implications for chronic neurodegenerative disease. Brain Behav Immun. 2004; 18:407–413. [PubMed: 15265532]

Sherer TB, Betarbet R, Kim JH, Greenamyre JT. Selective microglial activation in the rat rotenone model of Parkinson's disease. Neurosci Lett. 2003; 341:87–90. [PubMed: 12686372]

Shim KS, Lubec G. Drebrin, a dendritic spine protein, is manifold decreased in brains of patients with Alzheimer's disease and Down syndrome. Neurosci Lett. 2002; 324:209–212. [PubMed: 12009525]

Slomianka L, West MJ. Estimators of the precision of stereological estimates: an example based on the CA1 pyramidal cell layer of rats. Neuroscience. 2005; 136:757–767. [PubMed: 16344149]

Takahashi H, Sekino Y, Tanaka S, Mizui T, Kishi S, Shirao T. Drebrin-dependent actin clustering in dendritic filopodia governs synaptic targeting of postsynaptic density-95 and dendritic spine morphogenesis. J Neurosci. 2003; 23:6586–6595. [PubMed: 12878700]

Town T, Nikolic V, Tan J. The microglial "activation" continuum: from innate to adaptive responses. J Neuroinflammation. 2005; 2:24. [PubMed: 16259628]

Town T, Jeng D, Alexopoulou L, Tan J, Flavell RA. Microglia recognize double-stranded RNA via TLR3. J Immunol. 2006; 176:3804–3812. [PubMed: 16517751]

van den Pol AN. Viral infections in the developing and mature brain. Trends Neurosci. 2006; 29:398–406. [PubMed: 16806513]

Wang T, Town T, Alexopoulou L, Anderson JF, Fikrig E, Flavell RA. Toll-like receptor 3 mediates West Nile virus entry into the brain causing lethal encephalitis. Nat Med. 2004; 10:1366–1373. [PubMed: 15558055]

Weller M, Stevens A, Sommer N, Melms A, Dichgans J, Wietholter H. Comparative analysis of cytokine patterns in immunological, infectious, and oncological neurological disorders. J Neurol Sci. 1991; 104:215–221. [PubMed: 1940975]
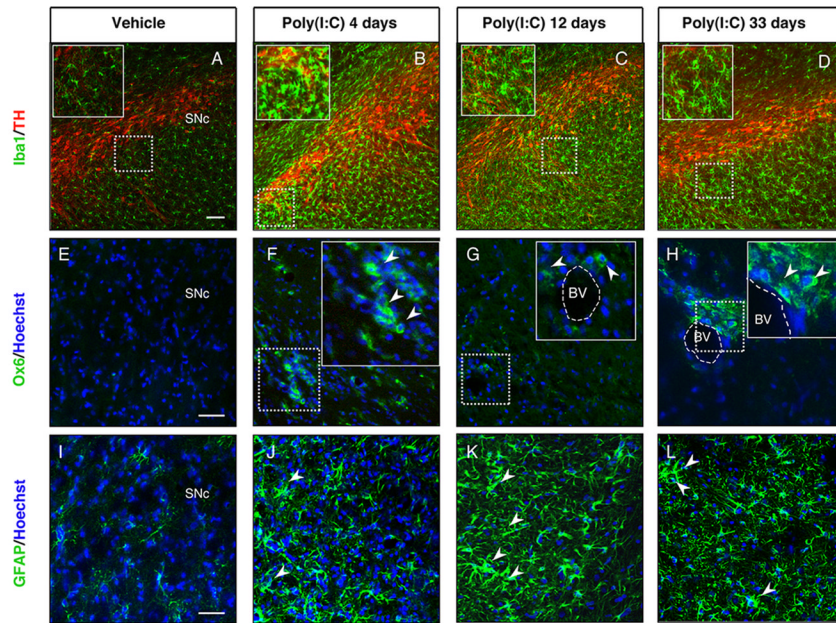
FIGURE 1. Intranigral injection of poly(I:C) induces microglial and astrocytic activation within the SN

Sprague Dawley rats were injected with vehicle or 20 μg poly(I:C) into the SN. Brains were isolated at 4, 12 and 33 days after injection and immunofluorescence microscopy was performed for TH (red), Iba1 (green), MHC class II antigen OX6 (green) and GFAP (green). **(A-D)** Iba1 immunohistochemistry revealed resting highly ramified microglia within the SN in vehicle-injected animals (A). In contrast, animals injected with poly(I:C) at 4, 12 and 33 days after the injection showed activated microglia with shorter and thicker processes and larger cell bodies (insets) (B-D). **(E-H)** MHC-II^{+} cells (arrowheads) were present in poly(I:C)-injected rats at 4,12 and 33 days after injection. **(I-L)** Astrocytic reaction (arrowheads) was found in the SN at 4, 12 and 33 days after poly(I:C) injection. Cell nuclei were counterstained with Hoechst. Dashed lines in F-H indicate blood vessels. Scale bar: 100 μm (A-D), 50 μm (E-L), 50 μm (insets B-D), 25 μm (insets F-H). BV Blood vessel, SNc Substantia nigra pars compacta.
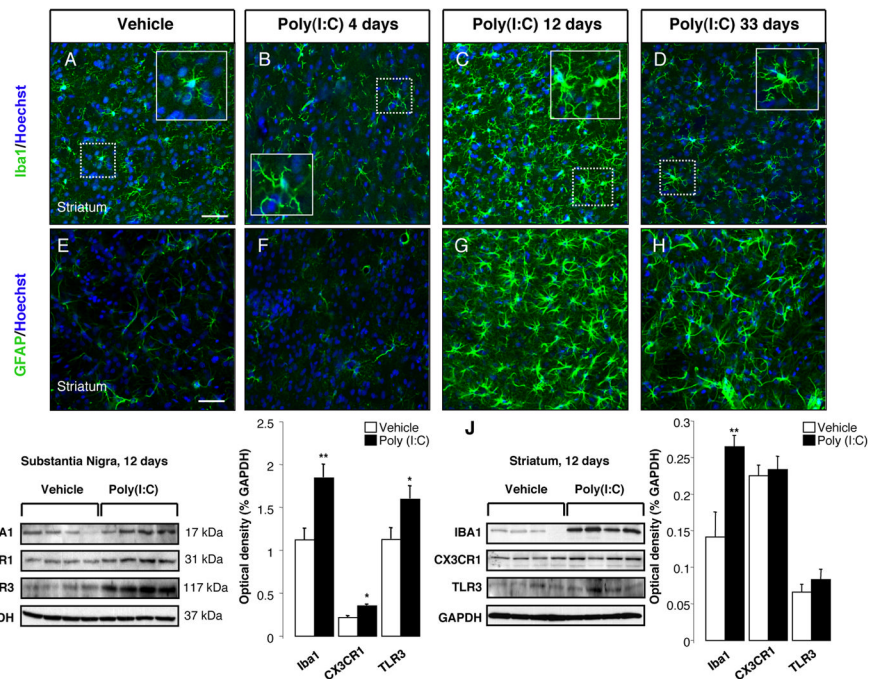
FIGURE 2. Intranigral injection of poly(I:C) induces microgliosis and astrocytic activation in the dorsolateral striatum

The dorsolateral striatum was immunostained for Iba1 (green) and GFAP (green) at 4,12 and 33 days after the intranigral injection of vehicle or 20 μg poly(I:C). Poly(I:C) promoted microglia activation **(A-D)** and astrocytic reaction **(E-H)** within the dorsolateral striatum starting at 12 days after the injection. At day 33, activated astrocytes were still present within the dorsolateral striatum (H) while microglial cells showed a resting phenotype (D). Cell nuclei were counterstained with Hoechst. Scale bar: 50 μm (A-H), 25 μm (insets A-D). **(I-J)** Western blots of SN and striatum extracts from vehicle and poly(I:C)-injected animals. Poly(I:C) injection induced an increase of the levels of Iba1, TLR3 and CX3CR1 in the SN. Levels of Iba1 were increased in the dorsolateral striatum. (Vehicle, n=9; poly(I:C), n=10; * p<0.05, ** p<0.01 unpaired t-test).
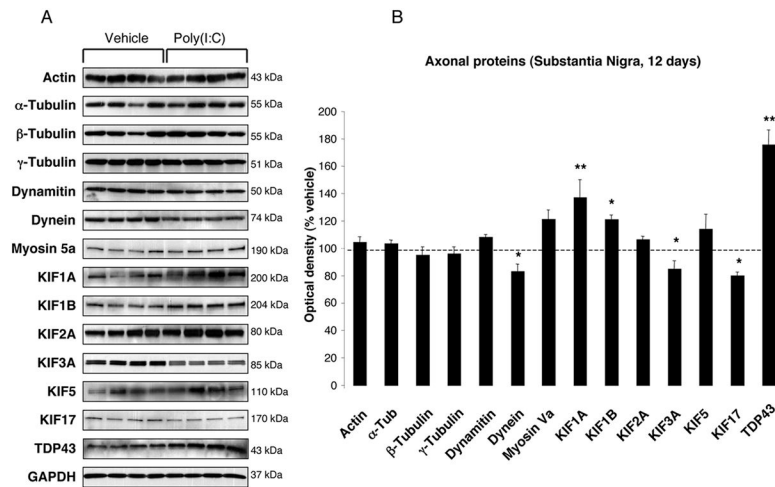
FIGURE 3. Nigral changes in the levels of axonal proteins at 12 days after poly(I:C) injection
(A) Anterograde transport motor proteins (KIF1A, KIF1B) were increased, whereas KIF3A, KIF17 and dynein were decreased. Levels of TDP-43 were increased. **(B)** Optical densities of the individual bands were quantified using NIH ImageJ. Optical densities were normalized by the averaged value of GAPDH and expressed as percentage of vehicle-injected conditions. Data are shown as mean ±SEM (Vehicle, n=9; poly(I:C), n=10; * p<0.05, ** p<0.01 unpaired t-test).
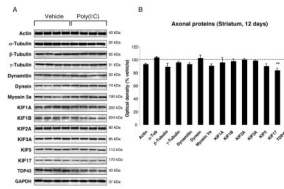
FIGURE 4. Striatal changes in the levels of axonal proteins at 12 days after poly(I:C) injection
(A) Poly(I:C) injection induced decreased levels of KIF17 and TDP-43. **(B)** Optical densities of the individual bands. Data are shown as mean ±SEM (Vehicle, n=9; poly(I:C), n=10; ** p<0.01 unpaired t-test).
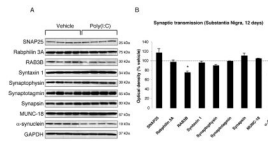
FIGURE 5. Nigral changes in the levels of synaptic proteins at 12 days after poly(I:C) injection
(A) Poly(I:C) injection induced decreased levels of RAB3B and α-Syn. **(B)** Optical densities of the individual bands. Data are shown as mean ±SEM (Vehicle, n=9; poly(I:C), n=10; * p<0.05, ** p<0.01 unpaired t-test).
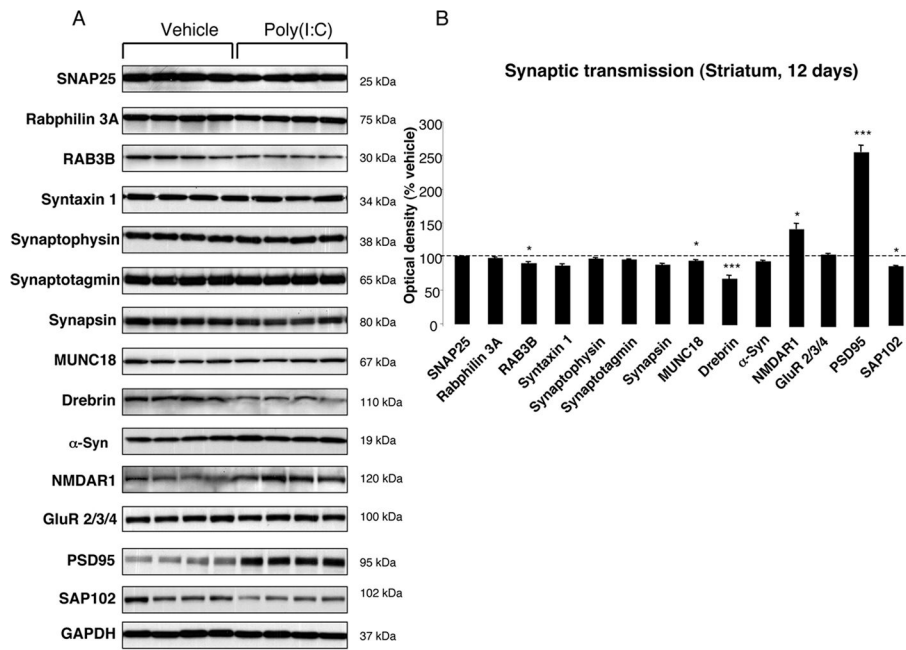
FIGURE 6. Striatal changes in the levels of synaptic proteins at 12 days after poly(I:C) injection
(A) Poly(I:C) injection induced decreased levels of RAB3B, MUNC18, Drebrin and SAP102. Levels of the postsynaptic proteins NMDAR1 and PSD-95 were significantly increased. (B) Optical densities of the individual bands. Data are shown as mean ±SEM (Vehicle, n=9; poly(I:C), n=10; *p<0.05, ** p<0.01, *** p<0.001 unpaired t-test).
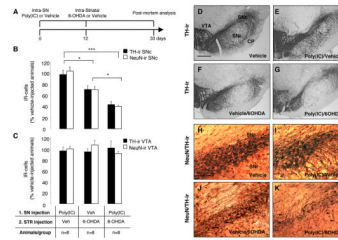
FIGURE 7. Poly(I:C) injection increases vulnerability to nigral DA neuron loss induced by low-dose 6-OHDA

(A) Experimental timeline: rats received a single intra-nigral injection of 20 μg poly(I:C) and 12 days later an intra-striatal injection of 5 μg 6-OHDA. The lesion was allowed to progress for 3 weeks after which animals were sacrificed for post mortem analyses. **(B)** Unbiased stereological analysis indicates that rats exposed to poly(I:C) injection, followed by a low-dose injection of 6-OHDA, had significant reduction of TH$^+$ neurons in the SNc when compared to animals injected with low-dose 6-OHDA. The loss of TH$^+$ neurons was reflected in the loss of NeuN$^+$ neurons, confirming true neuronal loss. Either vehicle or poly(I:C) injection alone did not induce neuronal cell loss. **(C)** Unbiased stereological analysis indicates no loss of TH$^+$ or NeuN$^+$ neurons in the VTA in any of the groups. **(D-G)** Images of TH immunohistochemistry from single coronal sections of rats injected with vehicle, poly(I:C) alone, 6-OHDA alone or combined insult. **(H-K)** Images of TH (brown) and NeuN (red) immunohistochemistry from single coronal sections of rats injected with vehicle, poly(I:C) alone, 6-OHDA alone or combined insult. Scale bar: 1.0 mm (D-G); 0.25 mm (H-K). SNc, substantia nigra pars compacta; SNr, substantia nigra pars reticulata; VTA, ventral tegmental area; CP, cerebral peduncle. Animals/group: vehicle/vehicle n=8, poly(I:C)/vehicle n=8, vehicle/6OHDA n=8, poly(I:C)/6OHDA n=8; * p<0.05, *** p<0.001, One-way Anova.
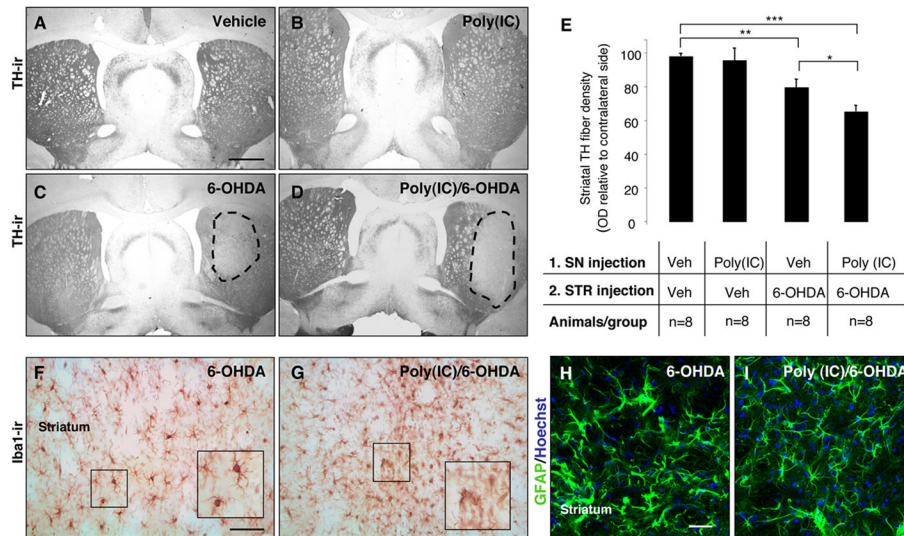
FIGURE 8. Intranigral injection of poly(I:C) increases the susceptibility of striatal DA nerve terminals to 6-OHDA toxicity

(**A-D**) Representative striatal sections stained for TH from rats treated with vehicle (A), 20 μg poly(I:C) (B), 5 μg 6-OHDA (C) and 20 μg poly(I:C) followed by 5 μg 6-OHDA injection (D). (**E**) Optical densitometric quantification of the TH-immunoreactive fibres in the striatum. The injection of 6-OHDA induced a significant loss of TH fibres in the striatum ($p \leq 0.001$). The volume of striatal TH$^+$ fibres in the 6-OHDA compared to poly(I:C)/6-OHDA treated rats, expressed relative to the unlesioned side, was significantly higher ($p \leq 0.01$). There was no difference between vehicle-treated rats and poly(I:C)-injected rats. (**F-G**) Immunohistochemistry against Iba1 in the striatum of 6-OHDA-lesioned and poly(I:C)/6-OHDA lesioned rats. Microglia in the striatum of poly(I:C)/6-OHDA lesioned rats showed activated morphology. (**H-I**) Immunohistochemical staining for GFAP (green) demonstrated similar astrocytic reaction in 6-OHDA-lesioned and poly(I:C)/6-OHDA lesioned rats. Scale bar, (A-D), 2.0 mm; (F-I), 50 μm. Animals/group: vehicle/vehicle n=8, poly(I:C)/vehicle n=8, vehicle/6OHDA n=8, poly(I:C)/6OHDA n=8; * $p<0.05$, ** $p<0.01$, *** $p<0.001$, One-way Anova.
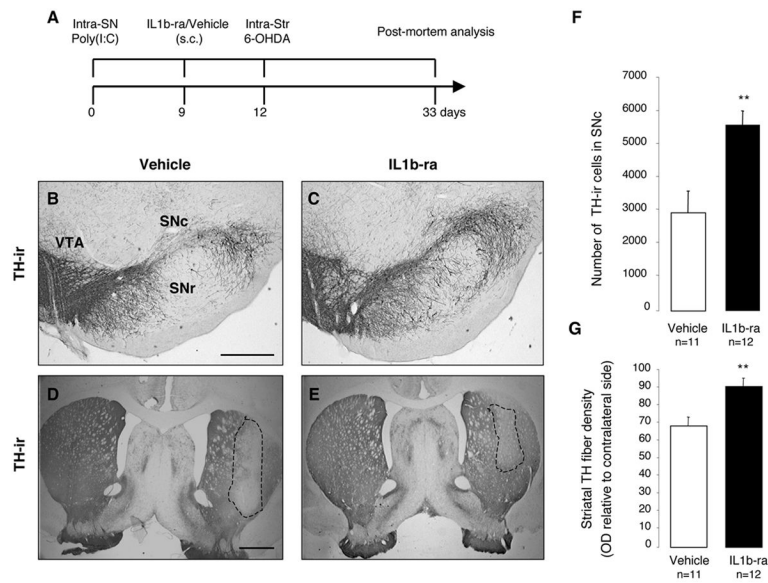
FIGURE 9. Neutralization of IL-1 reduces cell loss induced by poly(I:C) and 6-OHDA
(A) Experimental timeline: rats received a single intra-nigral injection of 20 μg poly(I:C) and 9 days later started on either IL-1ra or vehicle which continued through the experiment. All animals received an intra-striatal injection of 5.0 μg 6-OHDA 12 days after vehicle/ poly(I:C) injection and were allowed 21 days until post-mortem analyses. **(B-E)** Representative nigral and striatal sections stained for TH from rats treated with vehicle (B,D) or IL1-ra (C,E). **(F)** Stereological quantification TH$^+$ cells in the SNc revealed that IL1-ra prevented dopaminergic cell loss associated with poly(I:C) and 6-OHDA. **(G)** Optical densitometric quantification of the TH-immunoreactive fibres in the striatum revealed that IL1-ra prevented TH fibres loss in the striatum. Data are shown as mean ± SEM (Vehicle n=11, IL1-ra n=12; unpaired t-test, ** $p < 0.01$). Scale bar: (B-C), 0.25 mm; (D-E), 1.0 mm. SNc, pars compacta; SNr, pars reticulata; VTA, ventral tegmental area.

Table 1

Intranigral administration of poly(I:C) increases the level proinflammatory cytokines and chemokines.

Cytokine Chemokine	Substantia Nigra protein level 12 days post poly (IC) (pg/mg)	
	Vehicle	Poly (IC)
IL-1α	7.993 ± 1.558	**12.32 ± 1.208** *
IL-1β	5.564 ± 0.5115	6.183 ± 0.3726
IL-2	4.926 ± 0.7362	4.772 ± 0.3633
IL-4	5.910 ± 1.034	5.279 ± 0.4931
IL-6	55.19 ± 3.111	51.55 ± 2.167
IL-10	ND	ND
IFN-γ	6.618 ± 0.4500	8.275 ± 1.364
TNF-α	23.05 ± 3.670	25.25 ± 6.779
MCP-1	6.501 ± 0.9393	**9.541 ± 0.9878** *
MCD	1.959 ± 0.1989	2.195 ± 0.1701
Fractalkine	67.93 ± 3.127	69.00 ± 2.411
MIP-1α	10.12 ± 1.698	11.04 ± 1.224
MIP-2α	4.860 ± 0.6166	5.827 ± 0.5258
MIP-3α	96.18 ± 7.500	105.4 ± 7.355
RANTES	63.96 ± 3.495	**96.27 ± 5.275** **
TGF-β1	258.1 ± 24.64	246.1 ± 15.16

Cytokine Chemokine	Striatum protein level 12 days post poly (IC) (pg/mg)	
	Vehicle	**Poly (IC)**
IL-1α	13.29 ± 2.285	11.98 ± 1.279
IL-1β	4.728 ± 0.4303	**6.937 ± 0.5908** **
IL-2	5.124 ± 0.4348	5.790 ± 0.4551
IL-4	6.394 ± 0.9461	5.232 ± 0.4566
IL-6	95.59 ± 6.001	**114.5 ± 5.941** *
IL-10	ND	ND
IFN-γ	9.206 ± 2.411	9.822 ± 2.148
TNF-α	24.31 ± 4.697	**39.42 ± 3.461** *
MCP-1	2.174 ± 0.3089	**3.365 ± 0.3347** *
MCD	1.959 ± 0.1989	2.195 ± 0.1701
Fractalkine	142.8 ± 4.006	136.3 ± 3.928
MIP-1α	5.000 ± 0.5016	5.479 ± 0.5343
MIP-2α	4.228 ± 0.4588	4.770 ± 0.3614
MIP-3α	81.08 ± 4.540	86.95 ± 6.358
RANTES	73.06 ± 6.524	76.51 ± 7.677
TGF-β1	161.3 ± 10.06	**202.4 ± 5.722** **

Cytokine and chemokine levels were analysed in the SN and striatum at 12 days after poly (I:C) injection using multiplex ELISA. Poly(I:C) injection caused increased levels of IL-1α, MCP1 and RANTES within the SN and IL-1β, IL-6, TNF-α, MCP-1 and TGF-β in the striatum. Data are shown as mean ± SEM (vehicle, n=9; poly(I:C), n=10;

*
 $p < 0.05$

**
 $p < 0.001$ unpaired t-test).